Nigerian Journal of Pharmaceutical and Biomedical Research
Vol. 10 Issue.2 August, 2026. p-ISSN: 2579-1419 e-ISSN: 2814-1423

FINERENONE MITIGATES CISPLATIN-INDUCED NEPHROTOXICITY ASSOCIATED WITH SUPPRESSION OF NOX4/FERROPTOSIS AND NLRP3 INFLAMMASOME PATHWAYS IN RATS

Afrah Thiab Hlail

Department of Pharmacognosy and Medicinal Plants, College of Pharmacy, University of Thi-qar, Thi-qar 64001, Iraq
*Corresponding author E-mail: afrah.thiab@utq.edu.iq DOI 10.5281/zenodo.23954736

ABSTRACT

Cisplatin is a widely used chemotherapeutic agent whose clinical utility is limited by dose-dependent nephrotoxicity involving oxidative stress, ferroptosis, and inflammasome activation. Finerenone, a nonsteroidal mineralocorticoid receptor antagonist used in diabetic kidney disease, has, to our knowledge, not previously been tested in chemotherapy-induced kidney injury. Forty-eight adult male Wistar rats were assigned to six groups (n = 8 each): control, cisplatin (7.5 mg/kg, single intraperitoneal dose), finerenone alone (5 or 10 mg/kg/day, oral, 10 days), and cisplatin combined with each finerenone dose. Renal function, oxidative stress, ferroptosis-related markers, NLRP3 inflammasome-related markers, cytokines, apoptosis-related markers, and Nrf2/HO-1 expression were assessed 72 hours after cisplatin administration. Cisplatin produced marked renal dysfunction, oxidative injury, and changes in ferroptosis-, inflammasome-, and apoptosis-related markers relative to control. Finerenone co-administration attenuated these changes in a dose-dependent manner, with the high dose reducing serum creatinine by approximately 54% relative to cisplatin alone, and increased Nrf2 and HO-1 mRNA expression. Finerenone alone did not affect renal function markers. These findings indicate that finerenone confers dose-dependent nephroprotection against cisplatin-induced kidney injury in rats. This protection was associated with changes consistent with suppression of the NOX4-associated ferroptosis pathway and NLRP3 inflammasome activation, and with increased Nrf2/HO-1 mRNA expression, supporting further evaluation of finerenone as a candidate nephroprotective agent.

Keywords: *Cisplatin-induced nephrotoxicity, Ferroptosis, Finerenone, Mineralocorticoid receptor antagonist, NLRP3 inflammasome, Nrf2/HO-1 pathway*

1. INTRODUCTION

Cisplatin (cis-diamminedichloroplatinum II) remains one of the most widely used chemotherapeutic agents for solid tumors, but its clinical use is limited by nephrotoxicity, which occurs in a substantial proportion of treated patients (Tang *et al*., 2023; Vakilian *et al*., 2024). Mechanistically, cisplatin accumulates in renal proximal tubular cells and triggers DNA damage, mitochondrial dysfunction, endoplasmic reticulum stress, oxidative stress, and multiple forms of regulated cell death, together with a robust inflammatory response involving nuclear factor kappa B (NF-κB) and the NOD-, LRR-, and pyrin domain-containing protein 3 (NLRP3) inflammasome (Davoudi *et al*., 2022; Ren *et al*., 2024).

Ferroptosis, an iron-dependent form of regulated cell death driven by uncontrolled lipid peroxidation (Dixon and Olzmann, 2024), has emerged as a significant contributor to cisplatin-induced tubular injury, acting through pathways that intersect with NADPH oxidase (NOX)-

derived reactive oxygen species, glutathione depletion, and reduced glutathione peroxidase 4 (GPX4) activity (Li *et al*., 2023; Li *et al*., 2024). NADPH oxidase 4 (NOX4) is a major renal source of reactive oxygen species and has been implicated in kidney fibrosis (Thannickal *et al*., 2023). In addition, multiple natural and synthetic agents protect against cisplatin nephrotoxicity by suppressing ferroptosis through the nuclear factor erythroid 2-related factor 2/heme oxygenase-1 (Nrf2/HO-1) axis (Wang *et al*., 2022; Hu *et al*., 2025).

The NLRP3 inflammasome is independently activated by cisplatin and amplifies tubular injury through interleukin (IL)-1β and IL-18 release. Suppression of NLRP3 signaling attenuates renal injury in several rodent models, including cisplatin-induced and sepsis-induced kidney injury (Saad *et al*., 2024; Lu *et al*., 2024), and elevated urinary IL-18 is itself a validated early biomarker of acute kidney injury (Qin *et al*., 2022).

Finerenone is a highly selective, nonsteroidal mineralocorticoid receptor antagonist (MRA) that, unlike steroidal MRAs, achieves a more balanced tissue distribution and carries a lower risk of hyperkalemia (Okunlola *et al*., 2025). Beyond its established clinical benefit in diabetic kidney disease (Chen *et al*., 2023), where large outcome trials have reported reduced kidney and cardiovascular event rates (Filippatos *et al*., 2023), and in heart failure with mildly reduced or preserved ejection fraction (Solomon *et al*., 2024), finerenone has shown renoprotective, antioxidant, and anti-inflammatory effects in preclinical models of kidney injury, reducing oxidative stress and macrophage-driven inflammation (Piccirillo *et al*., 2023).

Although substantial preclinical evidence indicates that finerenone reduces oxidative stress and inflammation in ischemic and diabetic kidney injury (Savarese *et al*., 2024), to the best of our knowledge, no published study has evaluated finerenone in a chemotherapy-induced nephrotoxicity model or examined whether mineralocorticoid receptor (MR) antagonism modulates ferroptosis-related pathways, which are increasingly implicated in cisplatin nephrotoxicity (Li *et al*., 2023; Li *et al*., 2024). Given that the antioxidant effects of finerenone plausibly intersect with the NOX4–ferroptosis axis, and that MR antagonism has been associated with anti-inflammatory effects in other renal injury contexts (Piccirillo *et al*., 2023; Savarese *et al*., 2024), this represents a testable research question that, to our knowledge, has not been addressed.

We hypothesized that pretreatment with finerenone attenuates cisplatin-induced acute nephrotoxicity in rats, and this protection is associated with reduced NOX4-related oxidative stress and ferroptosis-related changes, reduced NLRP3 inflammasome activation, and increased Nrf2/HO-1 expression. Accordingly, the aim of this study was to evaluate the nephroprotective effect of finerenone against cisplatin-induced nephrotoxicity in rats and to explore associated changes in oxidative stress, ferroptosis-related markers, NLRP3 inflammasome-related markers, apoptosis-related markers, and Nrf2/HO-1 expression.

2. Materials and Methods

2.1 Experimental Animals

Adult male Wistar rats (8–10 weeks old, 200–250 g) were obtained from the Animal House, College of Pharmacy, University of Baghdad, and acclimatized for 7 days (12 h light/dark cycle, 22 ± 2 °C, standard chow and water *ad libitum*). Inclusion criteria were healthy animals with stable body weight during acclimatization; exclusion criteria were illness, weight loss > 10%, or abnormal baseline serum creatinine. The protocol was approved by College of pharmacy, University of Thi-Qar THPHREC202006-10 prior to initiation and conducted in accordance with the

ARRIVE 2.0 guidelines. Randomization was performed using a computer-generated random sequence, and outcome assessors were blinded to group allocation for all biochemical, ELISA, and RT-qPCR analyses.

2.2 Sample Size Justification

A priori sample size was estimated using G*Power software (effect size f = 0.6, α = 0.05, power = 0.80, six groups), which indicated a minimum of 6–7 animals per group; n = 8 per group was used to allow for anticipated 10–15% attrition.

2.3 Experimental Groups

Animals were randomized into six groups (n = 8/group; total N = 48):

- 1. Control (vehicle): oral gavage with 0.5% carboxymethyl cellulose (CMC) daily for 10 days + single intraperitoneal (i.p.) saline injection on day 8.
- 2. Cisplatin (CIS): vehicle gavage for 10 days + single i.p. cisplatin (7.5 mg/kg) on day 8.
- 3. Finerenone low-dose alone (FIN5): finerenone 5 mg/kg/day, oral gavage, for 10 days + i.p. saline on day 8.
- 4. Finerenone high-dose alone (FIN10): finerenone 10 mg/kg/day, oral gavage, for 10 days + i.p. saline on day 8.
- 5. CIS + FIN5: finerenone 5 mg/kg/day for 10 days + cisplatin 7.5 mg/kg i.p. on day 8.
- 6. CIS + FIN10: finerenone 10 mg/kg/day for 10 days + cisplatin 7.5 mg/kg i.p. on day 8.

Finerenone-alone groups (FIN5, FIN10) were included to exclude intrinsic nephrotoxicity of finerenone itself.

2.4 Drug/Toxicant Doses, Duration, and Routes

- Cisplatin (7.5 mg/kg, single i.p. dose): reported to produce reproducible acute tubular injury without excessive mortality (Tang *et al*., 2023).
- Finerenone (5 and 10 mg/kg/day, oral): selected to bracket the dose range reported to produce renoprotective and antioxidant effects in rat kidney-injury models (Piccirillo *et al*., 2023); finerenone was suspended in 0.5% CMC for oral gavage.
- Duration: finerenone/vehicle was administered daily for 10 days; cisplatin/saline was given once on day 8; animals were euthanized on day 11 (72 h post-cisplatin), a commonly used peak-injury time point (Tang *et al*., 2023).

2.5 Chemicals, Reagents, and Kits

- Cisplatin: Cytoplatin-50®, Cipla, India
- Finerenone: MedChemExpress, Monmouth Junction, NJ, USA, cat. no. HY-111372, purity ≥98%.
- Biochemical assay kits

Kits	Manufacturer	Country	Catalogue Number
Creatinine	Sigma-Aldrich	USA	MKA080
MDA	Elabscience	USA	E-EL-0060
GSH	Elabscience	USA	E-EL-0026
SOD	Elabscience	USA	E-EL-H1113
Labile Iron	Abcam	USA	Ab83366

- ELISA kits (NGAL, KIM-1, 4-HNE, IL-1β, IL-18, and TNF-α):

Kits	Manufacturer	Country	Catalogue Number
NGAL	Elabscience	USA	E-EL-R0662
KIM-1	Elabscience	USA	E-EL-R0568
4-HNE	Elabscience	USA	E-EL-0028
IL-1β	Elabscience	USA	E-EL-R0012
IL-18	Elabscience	USA	E-EL-R0567
T TNF-α	Elabscience	USA	E-EL-R2856

- RNA extraction (Trizol Reagent,Ivitrogen/ThermoFisher Scientific- USA,15596026), reverse-transcription (ThermoFisher Scientific- USA ,K1622) and qPCR reagents (Applied Biosystems, ThermoFisher Scientific- USA,A25742).

2.6 Sample Collection and Tissue Processing

On day 11 (72 h after cisplatin or saline administration), animals were euthanized under ketamine/xylazine anesthesia (ketamine 90 mg/kg and xylazine 10 mg/kg, intraperitoneally followed by cervical dislocation. Urine was collected over 12 h prior to sacrifice by placing rats individually in metabolic cages with free access to water but food deprived. Blood was collected by cardiac puncture (or retro-orbital sinus puncture) into non-anticoagulant tubes, left to clot for 30 min at room temperature, and serum was separated by centrifugation at 3000 rpm (or 2000 ×g) for 15 min at 4°C. until analysis. Kidneys were excised, rinsed immediately with ice-cold phosphate-buffered saline (PBS, pH 7.4) to remove excess blood, blotted dry on filter paper, and divided into two portions. The first portion was homogenized in ice-cold phosphate-buffered saline (PBS, pH 7.4) using a tissue homogenizer, centrifuged at 10,000 ×g for 15 min at 4°C, and the resulting supernatant was collected for biochemical assays and ELISA. Total protein concentration was determined using the Bradford assay (or Lowry method). The second portion was immediately snap-frozen in liquid nitrogen and stored for RNA extraction.

2.7 Outcome Measures

Outcome parameters were measured using three complementary analytical techniques (biochemical assays, ELISA, and RT-qPCR), consistent with standard practice in comparable nephroprotection studies (Khallaf *et al*., 2026).

2.7.1 Biochemical (colorimetric/kinetic) assays

- Serum creatinine and blood urea nitrogen (BUN), measured by standard kinetic colorimetric assay kits.
- Renal tissue malondialdehyde (MDA), measured by the thiobarbituric acid reactive substances (TBARS) colorimetric method.
- Reduced glutathione (GSH), measured by Ellman's colorimetric method.
- Superoxide dismutase (SOD) activity, measured by a standard colorimetric enzymatic assay kit.
- Renal tissue labile ferrous iron (Fe^{2+}) content, measured by a

ferrozine-based colorimetric assay (Li *et al*., 2024).

2.7.2 ELISA

- Urinary neutrophil gelatinase-associated lipocalin (NGAL) and kidney injury molecule-1 (KIM-1).
- 4-Hydroxynonenal (4-HNE) protein adducts, as a lipid-peroxidation marker.
- Pro-inflammatory cytokines IL-1β, IL-18, and tumor necrosis factor-α (TNF-α), expressed as pg/mg protein.

2.7.3 RT-qPCR (mRNA/gene expression)

All ferroptosis-, inflammasome-, and apoptosis-regulatory markers, as well as Nrf2 and HO-1, were assessed at the transcript level by RT-qPCR (Wang *et al*., 2022; Sabra *et al*., 2023). Protein expression of these targets was not assessed.

- GPX4 mRNA, as a ferroptosis-regulatory transcript.
- NOX4 mRNA, as the principal renal NADPH oxidase isoform.
- Acyl-CoA synthetase long-chain family member 4 (ACSL4) mRNA, as a ferroptosis-regulatory transcript.
- NF-κB (RelA) mRNA, as the principal inflammatory transcription-factor subunit driving NLRP3 pathway activation.
- NLRP3 mRNA, as the inflammasome sensor transcript.
- Caspase-1 (Casp1) mRNA, as the inflammasome effector transcript.
- Bax and Bcl-2 mRNA (Bax/Bcl-2 ratio), as apoptosis-regulatory transcripts.
- Caspase-3 (Casp3) mRNA, as the downstream apoptotic effector transcript.
- Nrf2 mRNA, as an antioxidant-pathway transcript.
- HO-1 mRNA, as an antioxidant-pathway transcript.

Total RNA was extracted, reverse-transcribed to cDNA, and amplified by qPCR as described in TRIzol reagent according to the manufacturer's protocol. RNA concentration and purity were assessed spectrophotometrically using a NanoDrop 2000 spectrophotometer (Thermo Fisher Scientific, USA) by measuring absorbance ratios at 260/280 nm and 260/230 nm. Reverse transcription was performed using RevertAid First Strand cDNA Synthesis Kit at 42°C for 60 min followed by enzyme inactivation at 70°C for 5 min. Real-time qPCR was performed on a StepOnePlus Real-Time PCR System (Applied Biosystems, USA) using PowerUp SYBR Green Master Mix. The thermocycling conditions consisted of initial denaturation at 95°C for 2 min, followed by 40 cycles of 95°C for 15 s and 60°C for 60 s. Relative mRNA expression for all targets was calculated using the comparative Ct ($2^{-\Delta\Delta Ct}$) method, with GAPDH as the reference gene. Primer sequences, amplicon sizes, and annealing temperatures are listed in Supplementary Table S1

Supplementary Table S1. Primer sequences for RT-qPCR

Gene (Rattus norvegicus)	Forward (5'→3')	Reverse (5'→3')	Amplicon (bp)	Annealing (°C)	Efficiency (%)
GAPDH (reference)	TGATTCTACCC ACGGCAAGT	AGCATCACCCCATTT GATGT	115	60	95-100
NOX4	TTCGCGGATCA CAGAAGGTC	AAGTTCAGGGCGTT CACCAA	142	60	95-100
NF-κB (RelA)	AGTCCCGCCCC TTCTAAAAC	CAATGGCCTCTGTGT AGCCC	106	60	95-100
NLRP3	CGAGACCTCTG GGAAAAAGCT	GCATACCATAGAGG AATGTGATGTACA	152	60	95-100
Casp1	GATGGCACATT TCCAGGACTGA	TGTTGCAGATAATG AGGGCAAGAC	138	60	95-100
Bax	TTTCATCCAGG ATCGAGCAG	AATCATCCTCTGCA GCTCCA	154	60	95-100
Bcl-2	GACTTTGCAGA GATGTCCAG	TCAGGTACTCAGTC ATCCAC	214	60	95-100
Casp3	ACTGGAATGTC AGCTCGCAA	GCAGTAGTCGCCTC TGAAGA	270	60	95-100
Nrf2 (Nfe2l2)	TTTGTAGATGA CCATGAGTCGC	TCCTGCCAAACTTGC TCCAT	161	60	95-100
HO-1 (Hmox1)	ATGTCCCAGGA TTTGTCCGA	ATGGTACAAGGAGG CCATCA	144	60	95-100
GPX4	GAGGCAAGACC GAAGTAAACT	CCCTGTACTTATCCA GGCAGA	165	60	95-100
ACSL4	TGGCTGGTTTCT GGTTGTTG	ACCTCCTCCGTTTCT TCTCC	158	60	95-100

2.8 Statistical Analysis

Each individual animal was considered an independent biological replicate (n = 8 per group). All assays were performed in triplicate, and technical replicates were averaged for each biological sample. Data were tested for normality (Shapiro–Wilk test) and homogeneity of variance (Levene's test). Normally distributed data were analyzed by one-way ANOVA with Tukey's post-hoc test; non-normally distributed data were analyzed using the Kruskal–Wallis test with Dunn's test. Data were tested for normality (Shapiro–Wilk test) and homogeneity of variance (Levene's test). Normally distributed data were analyzed by one-way ANOVA with Tukey's post-hoc test; non-normally distributed data were analyzed using the Kruskal–Wallis test with Dunn's post-hoc test. Data are expressed as mean ± SD. A two-tailed $p < 0.05$ was considered statistically significant. Statistical analyses were performed using using GraphPad Prism software (version 9.0, GraphPad Software, San Diego, CA, USA

3. Results

Because the finerenone-alone groups (FIN5 and FIN10) were included to exclude

intrinsic renal effects of finerenone, their data are presented for the renal function markers (Table 1, Figure 1). Tables 2–4 and Figures 2–6 present the mechanistic endpoints for the Control, CIS, CIS+FIN5, and CIS+FIN10 groups, which address the protective effect of finerenone against cisplatin. Mechanistic endpoints were not evaluated in the FIN5 and FIN10 per se groups, as their primary inclusion was to exclude intrinsic renal effects.

3.1 Finerenone Attenuates Cisplatin-Induced Renal Dysfunction

Cisplatin administration produced marked renal functional impairment relative to control, with serum creatinine rising from 0.45 ± 0.06 to 1.92 ± 0.28 mg/dL ($p < 0.001$), BUN rising from 18.2 ± 2.1 to 68.5 ± 7.4 mg/dL ($p < 0.001$), and urinary NGAL and KIM-1 each increasing approximately 12-fold (both $p < 0.001$ vs. control) (Table 1, Figure 1). Co-administration of finerenone attenuated all four markers in a dose-dependent manner: CIS+FIN5 reduced serum creatinine by approximately 30% and CIS+FIN10 by approximately 54% relative to CIS alone (both $p < 0.001$ vs. CIS; $p < 0.01$ between the two finerenone doses). Neither FIN5 nor FIN10 administered alone altered any renal function marker relative to control, indicating no evidence of intrinsic nephrotoxicity of finerenone at either dose on the basis of these markers.

Table 1. Renal function markers (biochemical assay and ELISA; mean ± SD, n = 8/group)

Group	Serum creatinine (mg/dL)	BUN (mg/dL)	Urinary NGAL (ng/mL)	Urinary KIM-1 (ng/mL)
Control	0.45 ± 0.06	18.2 ± 2.1	12.4 ± 3.0	0.8 ± 0.3
CIS	1.92 ± 0.28***	68.5 ± 7.4***	145.6 ± 18.2***	9.4 ± 1.6***
FIN5 alone	0.47 ± 0.05	18.9 ± 1.8	13.1 ± 2.7	0.9 ± 0.2
FIN10 alone	0.46 ± 0.07	19.1 ± 2.0	12.8 ± 2.9	0.8 ± 0.3
CIS + FIN5	1.34 ± 0.20###,‡	47.3 ± 5.9###,‡	92.7 ± 12.4###,‡	5.6 ± 1.1###,‡
CIS + FIN10	0.89 ± 0.15###	30.6 ± 4.2###	48.3 ± 9.6###	2.7 ± 0.7###

*Data are mean ± SD (n = 8/group). ***p < 0.001 vs. Control; ###p < 0.001 vs. CIS; ‡p < 0.01 CIS+FIN5 vs. CIS+FIN10. Approximate reduction in serum creatinine relative to CIS: FIN5 ≈ 30%, FIN10 ≈ 54%. CIS, cisplatin; FIN5/FIN10, finerenone 5/10 mg/kg/day; BUN, blood urea nitrogen; NGAL, neutrophil gelatinase-associated lipocalin; KIM-1, kidney injury molecule-1.*

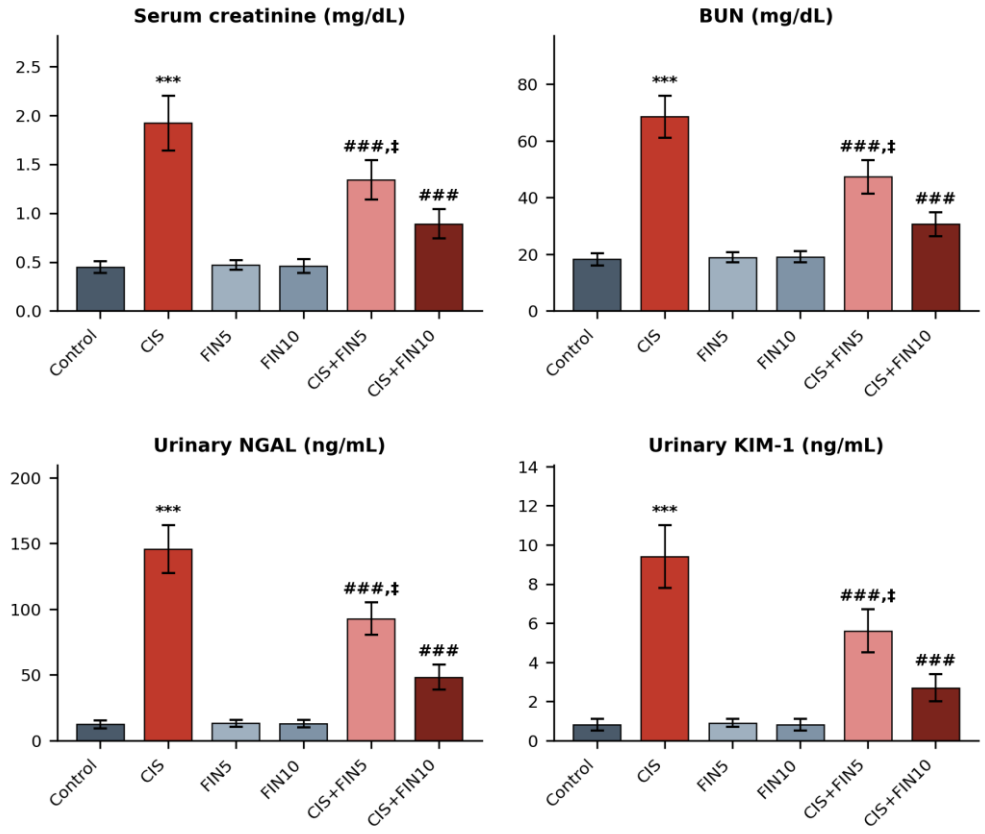

Figure 1. Finerenone attenuates cisplatin-induced renal functional impairment. Serum creatinine, blood urea nitrogen (BUN), and urinary neutrophil gelatinase-associated lipocalin (NGAL) and kidney injury molecule-1 (KIM-1) (ELISA) across the six experimental groups (Control, CIS, FIN5, FIN10, CIS+FIN5, CIS+FIN10). Bars represent mean ± SD (n = 8/group). ***p < 0.001 vs. Control; ###p < 0.001 vs. CIS; ‡p < 0.01 CIS+FIN5 vs. CIS+FIN10. CIS, cisplatin; FIN5/FIN10, finerenone 5/10 mg/kg/day. Data correspond to Table 1.

3.2 Finerenone Attenuates Cisplatin-Induced Oxidative Stress and Ferroptosis-Related Changes

Cisplatin increased tissue MDA, labile iron, and 4-HNE while depleting GSH and SOD activity (all $p < 0.001$ vs. control) (Table 2, Figure 2). At the transcript level, cisplatin suppressed GPX4 mRNA while markedly upregulating ACSL4 and NOX4 mRNA (all $p < 0.001$ vs. control), a pattern consistent with ferroptosis-related changes, although these markers alone do not establish ferroptotic cell death (Tables 2–3, Figure 3). Finerenone co-administration attenuated these changes dose-dependently: CIS+FIN10 increased GPX4 mRNA to 0.79 ± 0.10-fold of control ($p < 0.001$ vs. CIS), while reducing NOX4 and ACSL4 mRNA by approximately 60% and 58%, respectively, relative to CIS (both $p < 0.001$).

Table 2. Oxidative stress, ferroptosis-related, and antioxidant markers — biochemical assay, ELISA, and RT-qPCR (mean ± SD, n = 8/group)

Parameter (method)	Control	CIS	CIS + FIN5	CIS + FIN10
MDA, nmol/mg protein (biochemical)	2.1 ± 0.4	8.9 ± 1.2***	6.2 ± 0.9###,‡	3.6 ± 0.6###
GSH, µg/mg protein (biochemical)	24.5 ± 3.1	9.8 ± 1.7***	14.7 ± 2.0###,‡	19.9 ± 2.4###
SOD, U/mg protein (biochemical)	18.4 ± 2.2	7.1 ± 1.3***	10.9 ± 1.6###,‡	15.2 ± 1.9###
Labile iron, µmol/g tissue (biochemical)	1.2 ± 0.3	4.8 ± 0.7***	3.3 ± 0.5###,‡	2.0 ± 0.4###
4-HNE, ng/mg protein (ELISA)	3.0 ± 0.5	11.2 ± 1.6***	7.8 ± 1.1###,‡	4.6 ± 0.8###
GPX4 mRNA, fold vs. control (RT-qPCR)	1.00 ± 0.10	0.30 ± 0.07***	0.53 ± 0.08###,‡	0.79 ± 0.10###
NOX4 mRNA, fold vs. control (RT-qPCR)	1.00 ± 0.12	3.90 ± 0.55***	2.65 ± 0.40###,‡	1.55 ± 0.28###
Nrf2 mRNA, fold vs. control (RT-qPCR)	1.0 ± 0.15	1.6 ± 0.30*	2.4 ± 0.35###,‡	3.3 ± 0.42###

**p < 0.05, ***p < 0.001 vs. Control; ###p < 0.001 vs. CIS; ‡p < 0.01 CIS+FIN5 vs. CIS+FIN10. CIS, cisplatin; FIN5/FIN10, finerenone 5/10 mg/kg/day; MDA, malondialdehyde; GSH, reduced glutathione; SOD, superoxide dismutase; 4-HNE, 4-hydroxynonenal; GPX4, glutathione peroxidase 4; NOX4, NADPH oxidase 4; Nrf2, nuclear factor erythroid 2-related factor 2. Finerenone-alone groups are not shown for these endpoints.*

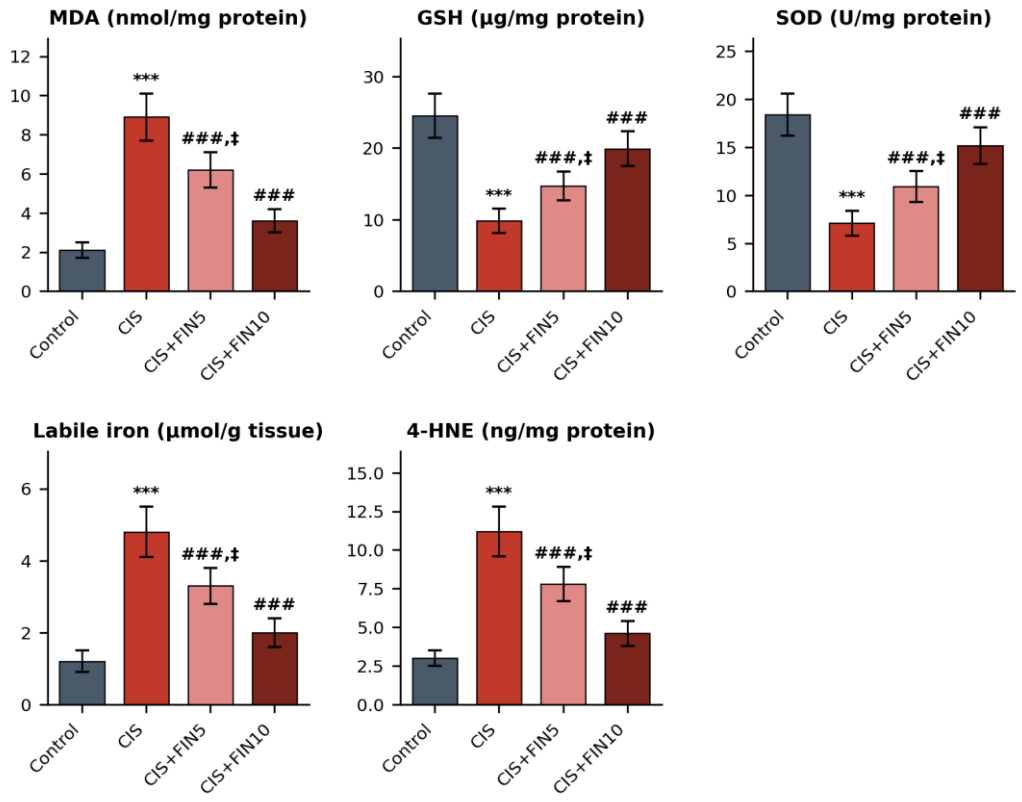

Figure 2. Finerenone reduces cisplatin-induced oxidative stress and lipid peroxidation. Tissue malondialdehyde (MDA), reduced glutathione (GSH), superoxide dismutase (SOD) activity, labile ferrous iron (Fe^{2+}) content, and 4-hydroxynonenal (4-HNE) protein adducts across Control, CIS, CIS+FIN5, and CIS+FIN10 groups. Bars represent mean ± SD (n = 8/group). ***p < 0.001 vs. Control; ###p < 0.001 vs. CIS; ‡p < 0.01 CIS+FIN5 vs. CIS+FIN10. CIS, cisplatin; FIN5/FIN10, finerenone 5/10 mg/kg/day. Data correspond to Table 2.

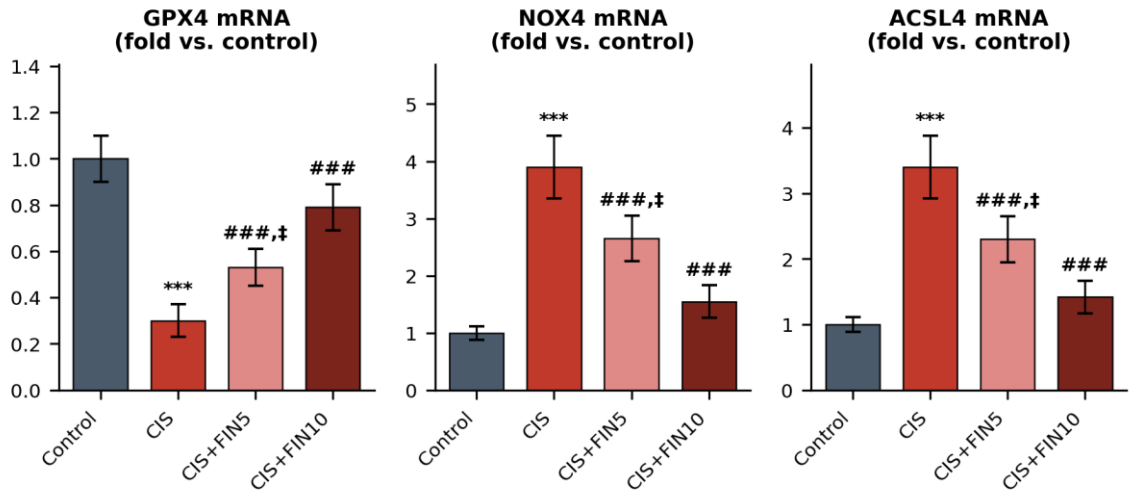

Figure 3. Finerenone modulates GPX4, NOX4, and ACSL4 mRNA expression. GPX4 (glutathione peroxidase 4), NOX4 (NADPH oxidase 4), and ACSL4 (acyl-CoA synthetase long-chain family member 4) mRNA (RT-qPCR, fold change vs. control) across Control, CIS, CIS+FIN5, and CIS+FIN10 groups. Bars represent mean ± SD (n = 8/group). ***p < 0.001 vs. Control; ###p < 0.001 vs. CIS; ‡p < 0.01 CIS+FIN5 vs. CIS+FIN10. CIS, cisplatin; FIN5/FIN10, finerenone 5/10 mg/kg/day. Data correspond to Tables 2–3.

3.3 Finerenone Reduces NLRP3 Inflammasome-Related Markers and Cytokine Levels

Cisplatin increased NF-κB (RelA), NLRP3, and caspase-1 mRNA expression 3.95–4.20-fold relative to control (all $p < 0.001$) (Table 3, Figure 4), with parallel increases in IL-1β, IL-18, and TNF-α (all $p < 0.001$ vs. control) (Table 4, Figure 4), consistent with inflammasome activation. Finerenone reduced all six markers dose-dependently; CIS+FIN10 lowered NLRP3 mRNA, caspase-1 mRNA, and IL-1β/IL-18/TNF-α to within approximately 1.5–2-fold of control values (all $p < 0.001$ vs. CIS).

Table 3. Ferroptosis-, inflammasome-, apoptosis-, and antioxidant-related gene expression — RT-qPCR (mRNA, fold change vs. control; mean ± SD, n = 8/group)

Gene (RT-qPCR)	Control	CIS	CIS + FIN5	CIS + FIN10
ACSL4	1.00 ± 0.11	3.40 ± 0.48***	2.30 ± 0.35###,‡	1.42 ± 0.25###
NF-κB (RelA)	1.00 ± 0.10	4.05 ± 0.53***	2.70 ± 0.39###,‡	1.60 ± 0.29###
NLRP3	1.00 ± 0.11	4.20 ± 0.55***	2.85 ± 0.40###,‡	1.75 ± 0.30###
Caspase-1 (Casp1)	1.00 ± 0.12	3.95 ± 0.52***	2.62 ± 0.37###,‡	1.58 ± 0.28###

Gene (RT-qPCR)	Control	CIS	CIS + FIN5	CIS + FIN10
Bax/Bcl-2 mRNA ratio	0.42 ± 0.08	3.15 ± 0.42***	2.02 ± 0.31###,‡	1.18 ± 0.22###
Caspase-3 (Casp3)	1.00 ± 0.13	5.40 ± 0.70***	3.35 ± 0.48###,‡	1.95 ± 0.33###
HO-1	1.0 ± 0.13	1.7 ± 0.29*	2.6 ± 0.36###,‡	3.5 ± 0.44###

**p < 0.05, ***p < 0.001 vs. Control; ###p < 0.001 vs. CIS; ‡p < 0.01 CIS+FIN5 vs. CIS+FIN10. Values are RT-qPCR mRNA fold change relative to control (control = 1.00), calculated using the comparative Ct ($2^{-\Delta\Delta Ct}$) method against the reference gene GAPDH; the Bax/Bcl-2 value is the ratio of Bax to Bcl-2 mRNA expression (control value 0.42) calculated by dividing the relative mRNA expression of Bax by that of Bcl-2 for each sample, with the control group normalized to 1.0 CIS, cisplatin; FIN5/FIN10, finerenone 5/10 mg/kg/day; ACSL4, acyl-CoA synthetase long-chain family member 4; NLRP3, NOD-, LRR-, and pyrin domain-containing protein 3; HO-1, heme oxygenase-1. GPX4, NOX4, and Nrf2 mRNA are reported in Table 2. Finerenone-alone groups are not shown for these endpoints (see Results, first paragraph).*

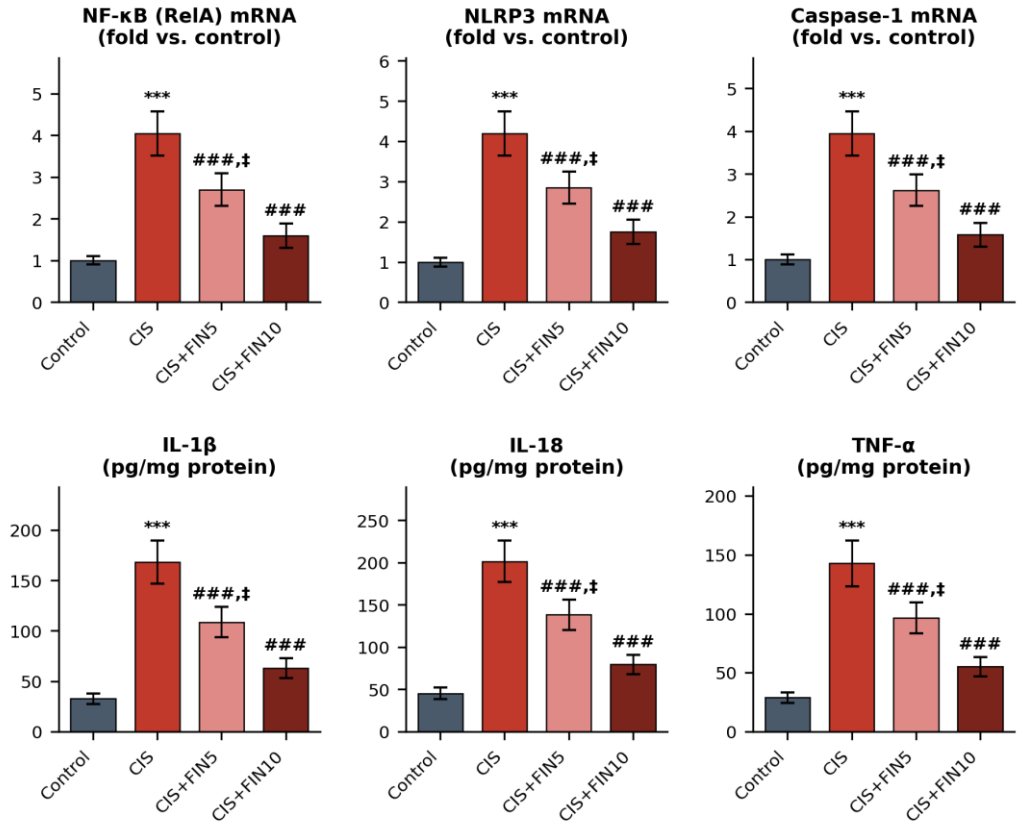

Figure 4. Finerenone reduces NLRP3 inflammasome-related markers and downstream cytokine levels. NF-κB (RelA), NLRP3, and caspase-1 mRNA (RT-qPCR, fold change vs. control) and IL-1β, IL-18, and TNF-α (ELISA, pg/mg protein) across Control, CIS, CIS+FIN5, and CIS+FIN10 groups. Bars represent mean ± SD (n = 8/group). ***p < 0.001 vs. Control; ###p < 0.001 vs. CIS; ‡p < 0.01 CIS+FIN5 vs. CIS+FIN10. CIS, cisplatin; FIN5/FIN10, finerenone 5/10 mg/kg/day; NF-κB, nuclear factor kappa B; NLRP3, NOD-, LRR-, and pyrin domain-containing protein 3; IL, interleukin; TNF-α, tumor necrosis factor-α. Data correspond to Tables 3–4.

Table 4. Inflammatory cytokines — ELISA (mean ± SD, pg/mg protein)

Cytokine (ELISA)	Control	CIS	CIS + FIN5	CIS + FIN10
IL-1β	32.6 ± 5.1	168.4 ± 21.3***	108.7 ± 15.2###,‡	62.9 ± 9.8###
IL-18	45.2 ± 6.8	201.5 ± 24.7***	138.2 ± 17.9###,‡	79.4 ± 11.3###

Cytokine (ELISA)	Control	CIS	CIS + FIN5	CIS + FIN10
TNF-α	28.9 ± 4.4	142.7 ± 19.5***	96.3 ± 13.1###,‡	55.1 ± 8.2###

****p < 0.001 vs. Control; ###p < 0.001 vs. CIS; ‡p < 0.01 CIS+FIN5 vs. CIS+FIN10. CIS, cisplatin; FIN5/FIN10, finerenone 5/10 mg/kg/day; IL, interleukin; TNF-α, tumor necrosis factor-α. Finerenone-alone groups are not shown for these endpoints (see Results, first paragraph).*

3.4 Finerenone Attenuates Cisplatin-Induced Changes in Apoptosis-Related Markers

Cisplatin increased the Bax/Bcl-2 mRNA ratio from 0.42 ± 0.08 to 3.15 ± 0.42 and caspase-3 mRNA 5.4-fold relative to control (both $p < 0.001$) (Table 3, Figure 5). Both markers were reduced dose-dependently by finerenone co-administration, reaching 1.18 ± 0.22 (Bax/Bcl-2 mRNA ratio) and 1.95 ± 0.33 (caspase-3 mRNA) in the CIS+FIN10 group (both $p < 0.001$ vs. CIS).

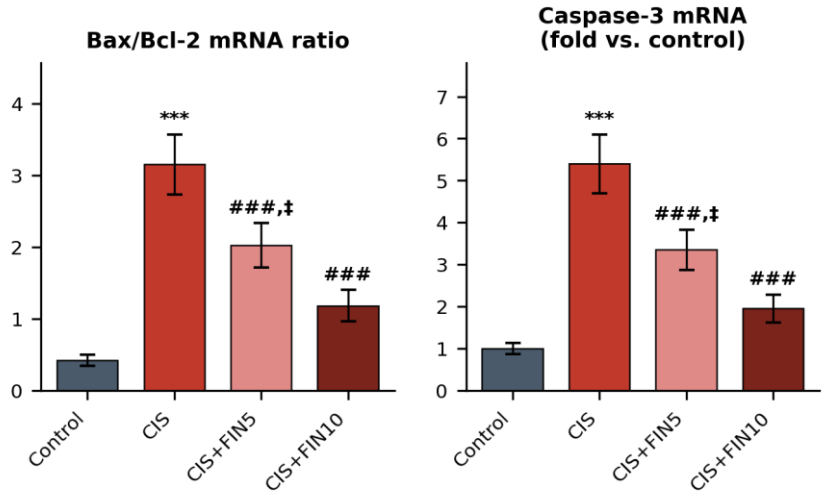

Figure 5. Finerenone attenuates cisplatin-induced changes in apoptosis-related markers. Bax/Bcl-2 mRNA ratio and caspase-3 mRNA (RT-qPCR; caspase-3 as fold change vs. control) across Control, CIS, CIS+FIN5, and CIS+FIN10 groups. Bars represent mean ± SD (n = 8/group). ***p < 0.001 vs. Control; ###p < 0.001 vs. CIS; ‡p < 0.01 CIS+FIN5 vs. CIS+FIN10. CIS, cisplatin; FIN5/FIN10, finerenone 5/10 mg/kg/day; Bax, Bcl-2-associated X protein; Bcl-2, B-cell lymphoma 2. Data correspond to Table 3.

3.5 Finerenone Co-Administration Is Associated with Increased Nrf2 and HO-1 mRNA Expression

Cisplatin alone produced a modest increase in Nrf2 and HO-1 mRNA relative to control (1.6- and 1.7-fold, respectively; $p < 0.05$) (Tables 2–3, Figure 6). Finerenone co-administration increased both markers further in a dose-dependent manner, with CIS+FIN10 reaching 3.3- and 3.5-fold of control values, respectively ($p < 0.001$ vs. CIS), consistent with an enhanced antioxidant transcriptional response. Protein-level expression and functional activity of this pathway were not assessed.

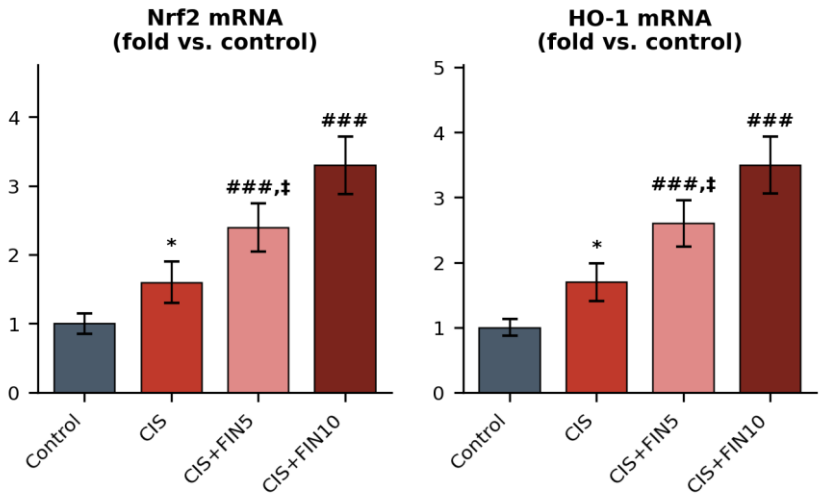

Figure 6. Finerenone increases Nrf2 and HO-1 mRNA expression. Nrf2 (nuclear factor erythroid 2-related factor 2) and HO-1 (heme oxygenase-1) mRNA (RT-qPCR, fold change vs. control) across Control, CIS, CIS+FIN5, and CIS+FIN10 groups. Bars represent mean ± SD (n = 8/group). *p < 0.05 vs. Control; ###p < 0.001 vs. CIS; ‡p < 0.01 CIS+FIN5 vs. CIS+FIN10. CIS, cisplatin; FIN5/FIN10, finerenone 5/10 mg/kg/day. Data correspond to Tables 2–3.

4. Discussion

In this rat model of cisplatin-induced acute kidney injury, finerenone conferred dose-dependent nephroprotection, evidenced by attenuated rises in serum creatinine, BUN, urinary NGAL, and KIM-1. This protection was accompanied by changes consistent with suppression of the NOX4-associated ferroptosis pathway (reduced NOX4 mRNA, increased GPX4 mRNA, and reduced ACSL4 mRNA, labile iron, MDA, and 4-HNE), by reduced NLRP3 inflammasome-related inflammation (reduced NLRP3 and caspase-1 mRNA and IL-1β, IL-18, and TNF-α levels), and by a lower Bax/Bcl-2 mRNA ratio and caspase-3 mRNA (Li *et al*., 2023; Saad *et al*., 2024). Although these markers are consistent with ferroptosis, they do not independently establish ferroptotic cell death. The parallel, dose-dependent increase in Nrf2 and HO-1 mRNA expression in finerenone-treated groups suggests that upregulation of this antioxidant pathway may contribute to the observed antioxidant and anti-ferroptotic changes, consistent with reports that finerenone reduces oxidative stress in other renal injury models (Savarese *et al*., 2024) and with the broader literature on Nrf2/HO-1-mediated nephroprotection against cisplatin (Wang *et al*., 2022). Because Nrf2/HO-1 expression and ferroptosis-related markers were assessed as parallel, correlative endpoints rather than through direct pathway inhibition or rescue experiments, this proposed mechanistic link should be regarded as hypothesis-generating rather than proven.

The pattern of antioxidant and anti-apoptotic changes is broadly comparable with that reported for sodium–glucose cotransporter 2 (SGLT2) inhibitors, another cardiorenal drug class with established kidney benefit in clinical trials (EMPA-KIDNEY Collaborative Group, 2023) and with antioxidant and anti-apoptotic nephroprotective effects against cisplatin nephrotoxicity in rats (Nishiyama and Kitada, 2023; Khallaf *et al*., 2026). Similar oxidative-stress and apoptotic mechanisms have also been described in cisplatin-induced hepatotoxicity (Ramadan *et al*., 2024).

To our knowledge, this is the first study to evaluate finerenone in a chemotherapy-induced nephrotoxicity model and the first

to suggest an association between nonsteroidal MR antagonism and ferroptosis-related changes in the kidney, extending the previously documented anti-inflammatory actions of finerenone in ischemic and diabetic kidney injury models (Piccirillo *et al*., 2023) to a distinct nephrotoxic insult and a distinct cell-death pathway. Because finerenone already has an established human safety and pharmacokinetic profile from cardiorenal indications (Solomon *et al*., 2024), these findings provide a preclinical rationale for future evaluation of finerenone as a nephroprotective adjunct during cisplatin-based chemotherapy; any such application would first require confirmation that finerenone does not compromise the antitumor efficacy of cisplatin.

Limitations. This study has several limitations. First, the major signaling molecules were assessed primarily at the mRNA level, without confirmation by Western blotting or immunohistochemistry; therefore, changes in protein expression, localization, and functional activity were not established. Second, direct ferroptosis inhibition or rescue experiments, and pathway-specific inhibition of NOX4, NLRP3, or Nrf2/HO-1, were not performed, so the reported relationships are associative rather than causal. Third, histopathological evidence of tubular injury is not presented. Fourth, only male rats were investigated, and sex-specific effects cannot be excluded. Fifth, a single cisplatin dose and a single time point (72 h after cisplatin) were examined. Finally, the possible effect of finerenone on the anticancer efficacy of cisplatin was not evaluated. Future studies incorporating protein-level validation, histopathology, ferroptosis-specific interventions, both sexes, and tumor-bearing models are warranted.

5. Conclusions

In this preclinical rat model, finerenone conferred dose-dependent nephroprotection against cisplatin-induced acute kidney injury, evidenced by attenuated rises in serum creatinine, BUN, urinary NGAL, and KIM-1. This protection was associated with changes consistent with suppression of the NOX4-associated ferroptosis pathway (increased GPX4 mRNA; reduced ACSL4 and NOX4 mRNA, labile iron, MDA, and 4-HNE), reduced NLRP3 inflammasome-related markers and IL-1β/IL-18/TNF-α levels, a lower Bax/Bcl-2 mRNA ratio and caspase-3 mRNA, and parallel increases in Nrf2 and HO-1 mRNA expression. These findings suggest a potentially novel mechanistic association between nonsteroidal mineralocorticoid receptor antagonism and ferroptosis-related pathways in the kidney, extending the known renoprotective profile of finerenone to a chemotherapy-induced nephrotoxicity model. Confirmation at the protein level, histopathological evaluation, and assessment of effects on cisplatin antitumor efficacy are required before clinical translation.

Conflict of Interest: The author declares no conflict of interest.

Funding: The author declares that this research received no external funding.

Data Availability Statement: The data that support the findings of this study are available from the corresponding author upon reasonable request.

Ethical Approval: This study was approved by College of pharmacy, University of Thi-Qar , approval number: THPHREC202006-10 and conducted in accordance with the ARRIVE 2.0 guidelines and institutional/national regulations on animal research. All institutional guidelines for the care and use of laboratory animals were strictly followed.

Author Contributions (CRediT): Conceptualization; Methodology; Investigation; Data curation; Formal analysis; Visualization; Writing – original draft; Writing – review & editing: Afrah

Thiab Hlail. The author approved the final version of the manuscript and agreed to be accountable for all aspects of the work.

References

Chen, W., Zheng, L., Wang, J., Lin, Y., and Zhou, T. (2023). Overview of the safety, efficiency, and potential mechanisms of finerenone for diabetic kidney diseases. *Frontiers in Endocrinology*, 14, 1320603.

Davoudi, M., Jadidi, Y., Moayedi, K., Farrokhi, V., and Afrisham, R. (2022). Ameliorative impacts of polymeric and metallic nanoparticles on cisplatin-induced nephrotoxicity: A 2011–2022 review. *Journal of Nanobiotechnology*, 20, 504.

Dixon, S. J., and Olzmann, J. A. (2024). The cell biology of ferroptosis. *Nature Reviews Molecular Cell Biology*, 25, 424–442.

EMPA-KIDNEY Collaborative Group, Herrington, W. G., Staplin, N., Wanner, C., Green, J. B., Hauske, S. J., *et al*. (2023). Empagliflozin in patients with chronic kidney disease. *New England Journal of Medicine*, 388(2), 117–127.

Filippatos, G., Anker, S. D., August, P., Coats, A. J. S., Januzzi, J. L., Mankovsky, B., Rossing, P., Ruilope, L. M., Pitt, B., Sarafidis, P., Teerlink, J. R., Kapelios, C. J., Gebel, M., Brinker, M., Joseph, A., Lage, A., Bakris, G., and Agarwal, R. (2023). Finerenone and effects on mortality in chronic kidney disease and type 2 diabetes: A FIDELITY analysis. *European Heart Journal - Cardiovascular Pharmacotherapy*, 9(2), 183–191.

Hu, J., Zhang, Y., Zhang, Y., Shi, N., Miu, Y., Huang, J., *et al*. (2025). Bergenin inhibits ferritinophagy and ferroptosis in cisplatin-induced acute kidney injury by activating the p-GSK3beta/Nrf2/PPARgamma pathway. *International Immunopharmacology*, 147, 114004.

Khallaf, E. K., Ramadan, E. A., Elmazar, M. M., and Safar, M. M. (2026). Dapagliflozin attenuates cisplatin-induced nephrotoxicity in rats through modulation of ROS/NF-κB, BCL2/Bax and PINK1/Parkin signaling pathways. *Scientific Reports*, 16, 15227.

Li, P., Li, D., Lu, Y., Pan, S., Cheng, F., Li, S., Zhang, X., Huo, J., Liu, D., and Liu, Z. (2024). GSTT1/GSTM1 deficiency aggravated cisplatin-induced acute kidney injury via ROS-triggered ferroptosis. *Frontiers in Immunology*, 15, 1457230.

Li, Y., Li, K., Zhao, W., Wang, H., Xue, X., Chen, X., *et al*. (2023). VPA improves ferroptosis in tubular epithelial cells after cisplatin-induced acute kidney injury. *Frontiers in Pharmacology*, 14, 1147772.

Lu, J., Hou, Y., Liu, S. X., Jin, B., Liu, J., Li, N., Zhu, Y., Zhang, Q. Y., Wan, C., Feng, Y., Xie, J., and Jiang, C. M. (2024). Acetyl-CoA synthetase 2 induces pyroptosis and inflammation of renal epithelial tubular cells in sepsis-induced acute kidney injury by upregulating the KLF5/NF-κB pathway. *Cell Communication and Signaling*, 22, 1–15.

Nishiyama, A., and Kitada, K. (2023). Possible renoprotective mechanisms of SGLT2 inhibitors. *Frontiers in Medicine*, 10, 1115413.

Okunlola, A. O., Kolawole, O., Otabor, E., Hassan, A., Hamilton, M., Alomari, L., Lam, J., and Idowu, A. B. (2025). Cardiovascular outcomes and hyperkalemia risk in patients with diabetes, chronic kidney disease and heart failure: A real-world comparison of non-steroidal versus steroidal mineralocorticoid receptor antagonists. *Cureus*, 17(11), e97588.

Piccirillo, F., Liporace, P., Nusca, A., Nafisio, V., Corliano, A., Magaro, F., Antonelli Incalzi, R., Ussia, G. P., and Grigioni, F. (2023). Effects of finerenone on cardiovascular and chronic kidney diseases: A new weapon against cardiorenal morbidity and mortality—A comprehensive review. *Journal of Cardiovascular Development and Disease*, 10, 236.

Qin, Z., Li, H., Jiao, P., Jiang, L., Geng, J., Yang, Q., Liao, R., and Su, B. (2022). The value of urinary interleukin-18 in predicting acute kidney injury: A systematic review and meta-analysis. *Renal Failure*, 44(1), 1717–1727.

Ramadan, O. I., Ali, L. S., Abd-Allah, F. M., Ereba, R. E. A., Humeda, H. S., Damanhory, A. A., Moustafa, A. E., Younes, A. M., Awad, M. M. Y., and Omar, N. A. A. (2024). Co-administration of either curcumin or resveratrol with cisplatin treatment decreases hepatotoxicity in rats via anti-inflammatory and oxidative stress-apoptotic pathways. *PeerJ*, 12, e17687.

Ren, N., Wang, W. F., Zou, L., Zhao, Y. L., Miao, H., and Zhao, Y. Y. (2024). The nuclear factor kappa B signaling pathway is a master regulator of renal fibrosis. *Frontiers in Pharmacology*, 14, 1335094.

Saad, H. M., Elekhnawy, E., Shaldam, M. A., Alqahtani, M. J., Altwaijry, N., Attallah, N. G. M., *et al*. (2024). Rosuvastatin and diosmetin inhibited the HSP70/TLR4/NF-κB p65/NLRP3 signaling pathways and switched macrophage to M2 phenotype in a rat model of acute kidney injury induced by cisplatin. *Biomedicine & Pharmacotherapy*, 171, 116151.

Sabra, M. S., Hemida, F. K., and Allam, E. A. H. (2023). Adenine model of chronic renal failure in rats to determine whether MCC950, an NLRP3 inflammasome inhibitor, is a renopreventive. *BMC Nephrology*, 24, 377.

Savarese, G., Lindberg, F., Filippatos, G., Butler, J., and Anker, S. D. (2024). Mineralocorticoid receptor overactivation: Targeting systemic impact with non-steroidal mineralocorticoid receptor antagonists. *Diabetologia*, 67, 246–262.

Solomon, S. D., McMurray, J. J. V., Vaduganathan, M., Claggett, B., Jhund, P. S., Desai, A. S., *et al*. (2024). Finerenone in heart failure with mildly reduced or preserved ejection fraction. *New England Journal of Medicine*, 391(16), 1475–1485.

Tang, C., Livingston, M. J., Safirstein, R., and Dong, Z. (2023). Cisplatin nephrotoxicity: New insights and therapeutic implications. *Nature Reviews Nephrology*, 19(1), 53–72.

Thannickal, V. J., Jandeleit-Dahm, K., Szyndralewiez, C., and Torok, N. J. (2023). Pre-clinical evidence of a dual NADPH oxidase 1/4 inhibitor (setanaxib) in liver, kidney and lung fibrosis. *Journal of Cellular and Molecular Medicine*, 27(4), 471–484.

Vakilian, A., Mohammadi, S., Shokri, F., Maleki, M., Kheiry, M., Kheiri, A. (2024). The renin-angiotensin system involvement in cisplatin-induced nephrotoxicity: An overview of physiological and pathological mechanisms—A systematic review. *International Journal of Nephrology*, 2024, 1511216.

Wang, S., Zheng, Y., Jin, S., Fu, Y., and Liu, Y. (2022). Dioscin protects against cisplatin-induced acute kidney injury by reducing ferroptosis and apoptosis through activating Nrf2/HO-1 signaling. *Antioxidants*, 11(12), 2443.